Performance based out-of-plane posttensioning seismic retrofit design of unreinforced masonry walls

N. Ismail & J. M. Ingham

University of Auckland, New Zealand.

P. T. Laursen

California Polytechnic State University, San Luis Obispo, United States.

2010 NZSEE Conference

ABSTRACT: A performance based design procedure was developed based on the out-of-plane flexural testing of seismically retrofitted unreinforced masonry (URM) walls using posttensioning. A macro level single degree of freedom (SDOF) dynamic model for the retrofit design of URM walls was developed. The test walls were dynamically tested by exciting the walls with a hammer and the developed model was updated to match the actual dynamic response of the tested walls. The developed SDOF model was used to find the pushover capacity curve for the posttensioned walls. The New Zealand Loading Standard's (NZS 1170) defined elastic site spectrum was used to develop the demand spectra. Consequently, a simplified demand-capacity phase diagram was developed to study the seismic behaviour of posttensioned walls and was used to analyse the tested posttensioned URM wall. Using the graphically aided analysis, seismic performance of the wall was investigated and it was inferred that the simplified analysis procedure can be used for performance based posttensioning seismic retrofit design of New Zealand URM buildings.

1 INTRODUCTION

Structural analysis in earthquake engineering is a delicate task that requires a high level of sophistication associated with the input response histories of ground motions and with the detailed hysteretic non-linear behaviour of structural elements. A detailed non-linear dynamic analysis of a URM structure is considered computationally expensive and labour intensive (Ismail et al. 2009b). Conversely, seismic analysis procedures specified in some building codes are based on linear elastic structural behaviour that fail to predict quantitative damage. In the design procedure presented herein non-linear static analysis (NSA) of a simplified (macro level) analytical model was performed and the seismic response of the structure was graphically depicted as a demand-capacity phase diagram (DCPD).

Previously the NSA procedure was presented for planar structures and moment resisting frames, with the concept first presented by Freeman et al. (1975) and further refined by several researchers (Chopra and Goel 1999; Freeman 1998; Fajfar 2000;) and being introduced into many building codes (ATC 1996; CEN 1998). The existing simplified non-linear procedure was adapted for posttensioning seismic retrofit design of New Zealand URM buildings and is believed to be superior to its counterpart elastic analysis approach due to its ability to depict the expected level of damage and displacement for URM buildings. A three dimensional (3D) dynamic analysis can be used to find the most critically stressed elements of the structure and then a two dimensional (2D) planer NSA can be performed to predict the performance of the critical structural element (Mogadam and Tso 2000). In order to develop a precise simplified mathematical model, the structural dynamic characteristics of posttensioned URM walls was investigated in an experimental study as described in Section 2.

2 EXPERIMENTAL STUDY

2.1 Test wall specifications

Wall dimensions are specified in Table 1. The two posttensioned walls PTB-01 and PTS-02 had the same geometry as that of the non-retrofitted wall, C-01. More details pertaining to the selection of wall geometry, material properties, boundary conditions and level of applied prestress were presented in Ismail et al. (2009a).

Table 1. Wall dimensions and properties

Wall	Effective height h_e (mm)	Length l_w (mm)	Thickness t (mm)	Wall self-weight N_w (kN)	Masonry strength f'_m (MPa)	Tendon type	Initial pre-stress		Bearing stress f_m[a]/f'_m (ratio)
							P (kN)	f_{ps} (MPa)	
C-01	3900	1170	220	19	5.3	-	-	-	-
PTB-01	3900	1170	220	19	5.3	B[b]	50	442	0.32
PTS-02	3900	1170	220	19	5.3	S[c]	100	789	0.56

[a] $f_m = (N_w+P)/(A_b)$ where A_b is the area of bearing plate
[b] Threaded mild steel bar (f_{py} = 500 MPa)
[c] Sheathed, greased high strength seven-wire strand (f_{py} = 1300 MPa)

2.2 Test Wall Construction

The walls were constructed using a common bond pattern, with one header course after every three stretcher courses, by an experienced brick layer under supervision. Vintage clay bricks recycled from an 1880's old URM building, being 220 mm × 110 mm × 90 mm in size, were laid with roughly 15 mm thick mortar courses. A flexible 50 mm conduit was used in PTB-01 and PTS-02 to form a cavity during construction, and bricks were accordingly chiselled to accommodate the conduit. As there was no bond between masonry and posttensioned tendon, the conduit encased tendons behaved as if they were placed in a cored cavity. From discussions with specialised local construction contractors it was identified that for seismic retrofit of URM buildings, current techniques are capable of drilling a core cavity up to four stories with a precision of ±10 mm.

2.3 Material Properties

Average URM material properties were determined by material testing consistent with ASTM standards, typically in sets of three samples. Masonry compressive strength f'_m and masonry elastic modulus E_m were determined by testing three brick high prisms and mortar compressive strength f'_j was determined by testing three 50 mm × 50 mm cubes subjected to compression loading. Masonry cohesion c and coefficient of friction μ were investigated by bed joint shear testing of 6 three brick high prisms with varying axial compression applied using externally posttensioned high strength bars. Table 2 reports the material properties and Figure 1 shows photographs of the testing.

Table 2. Material properties

	f'_m (MPa)	E_m (GPa)	f'_j (MPa)	c (MPa)	μ
Mean Value	5.3	2.8	1.6	0.1	0.46

Figure 1. Photographs of material testing

For wall PTB-01 a threaded mild steel 12 mm diameter bar with a tensile yield strength f_{py} of 500 MPa was used with couplers (incl. flat base hexagonal nut and bearing plate at both ends of the tendon) as end anchorages and for wall PTS-02 a seven-wire prestressing strand with 12.7 mm diameter, greased and sheathed, with a nominal tensile yield strength f_{py} of 1300 MPa was used. In order to make the posttensioning reversible and accommodate strand removal (which is an architectural requirement for historic seismic retrofit), a 50 mm thick mild steel plate split in two halves was used, which can be removed to destress the strand. Test wall PTB-01 was posttensioned using a 100 kN hydraulic jack which was removed after tightening the nut to clasp the posttensioning

bar. For test wall PTS-02 an electronic hydraulic jack was used to apply the initial posttensioning force and the taut strand was anchored with a barrel and wedges. Prestress levels detailed in Table 1 were ensured by applying the required stress immediately before testing.

2.4 Pseudo-Static Tests

The walls specified in Table 1 were tested for out-of-plane stability using a pseudo-static test setup as shown in Figure 2. Test wall PTS-02 did not reach its ultimate flexural capacity before the test was stopped due to safety concerns and test wall PTB-01 was loaded up to its flexural capacity.

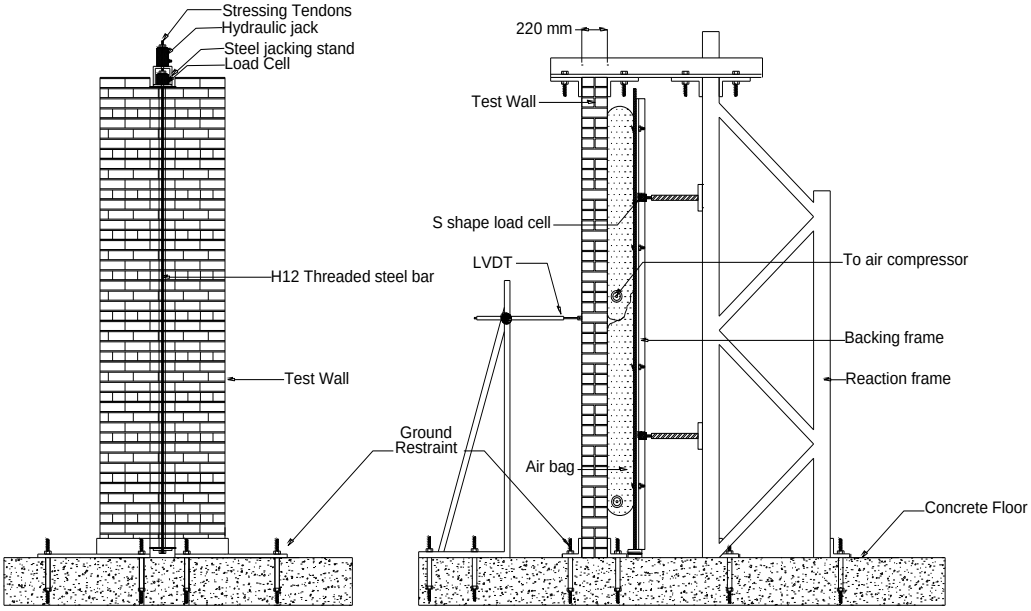

(a) Front view (b) Side view

Figure 2. Test setup for pseudo-static out-of-plane testing

Figure 3 shows the force-displacement histories for the test walls. A single large crack at or near mid-height and no flexural distributed cracks were observed in both wall tests. In wall PTB-01 the threaded mild steel bar reached its elastic limit and yielded, causing strength degradation, but no visible residual displacements were observed. A gradual ductile failure mode was observed in wall PTS-02 with no residual displacement and strand stress did not exceed the specified elastic limit. More details of this testing were presented in Ismail et al. (2009a).

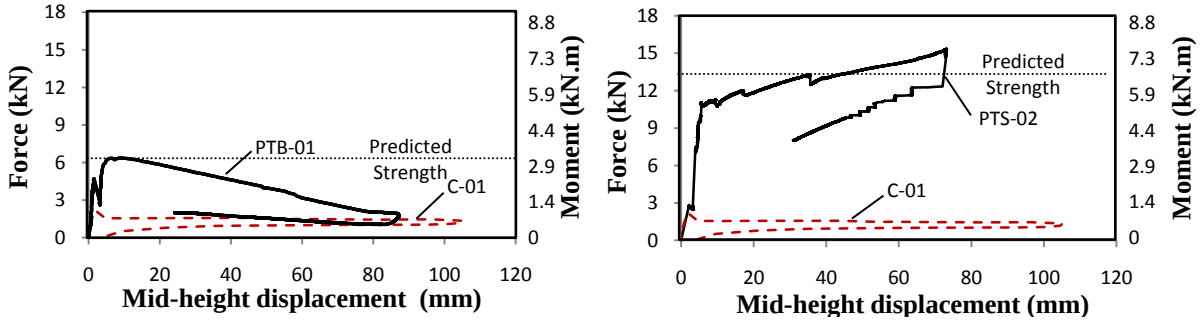

(a) PTB-01 and C-01 (b) PTS-02 and C-01

Figure 3. Test results for psuedo-static out-of-plane testing

The test walls' performance, when subjected to face loading, is summarized in Table 3 where V_u is the value of maximum total lateral force measured through load cells and M_u is the corresponding maximum recorded moment applied at mid-height. Total applied force and moment when first crack appeared were denoted by V_c and M_c respectively. The ultimate displacement capacity was defined as $\gamma_u = d_u/h_{eff}$, where the ultimate displacement d_u was quantified by the measured displacement at mid-height location when lateral strength had degraded below 80% of measured flexural capacity, and h_{eff}

is the effective height of the wall. Flexural capacities at cracking (M_c) and ultimate strength levels (M_n) were predicted using Equations 4 and 5 as advocated by Popehn et al. (2008) and were compared with experimental values as denoted by the dotted lines in Figure 3.

Table 3. Test results

Wall	Predicted values				Actual values				γ_u (%)	Comments
	V_c (kN)	V_n (kN)	M_c (kN.m)	M_n (kN.m)	V_c (kN)	V_u (kN)	M_c (kN.m)	M_u (kN.m)		
C-01*	-	-	-	-	-	2.2	2.1	2.1	6.0	Crack at mid-height
PTB-01	4.2	6.6	2.1	3.2	4.6	6.3	2.2	3.1	1.6	Crack at mid-height, bar yielded
PTS-02	6.5	13.0	3.2	6.4	10.8	>15.3	5.2	>7.4	4.0	Crack at mid-height

*Tested in a concurrent study and reported in Derakhshan et al. (2010)

2.5 Dynamic Tests

Testing of the posttensioned walls was conducted using the test setup shown in Figure 4, consisting of accelerometers and a data acquisition system. A hammer was used to apply impact and induce excitations in the posttensioned walls and the dynamic response was quantified by the voltage output which was further used to form a fourier transform and power spectra.

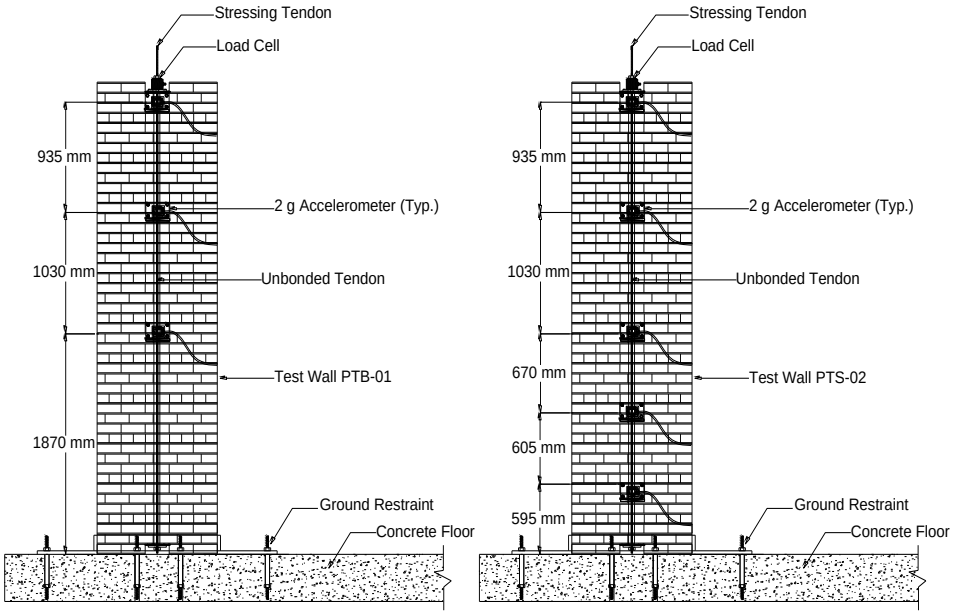

(a) PTB-01 **(b) PTS-02**

Figure 4. Test setup for dynamic testing

Dynamic properties acquired through this testing were used for the development of an updated SDOF computer model that was analysed using the modal response spectrum method in a finite element based computer package. The natural frequencies in the elastic range and the model assurance criteria were matched such that the SDOF model accurately replicated the measured elastic dynamic response of the walls. Equation 1 mathematically represents a linear elastic system where: *M*, *C* and *K* are mass, damping and stiffness system matrices respectively; $\ddot{y}(t)$, $\dot{y}(t)$ and $y(t)$ are acceleration, velocity and displacement respectively and $F(t)$ is the force applied to the system.

$$M\ddot{y}(t) + C\dot{y}(t) + Ky(t) = F(t) \quad (1)$$

For lightly damped structures, the eigen-value problem can be solved to determine frequencies and mode shapes using Equation 2

$$(K - \Omega M)\phi = 0 \quad (2)$$

where Ω and ϕ are matrices of square of the frequencies and the mode shapes. Figure 5 and 6 shows the response of the walls in terms of power spectra and fourier transform.

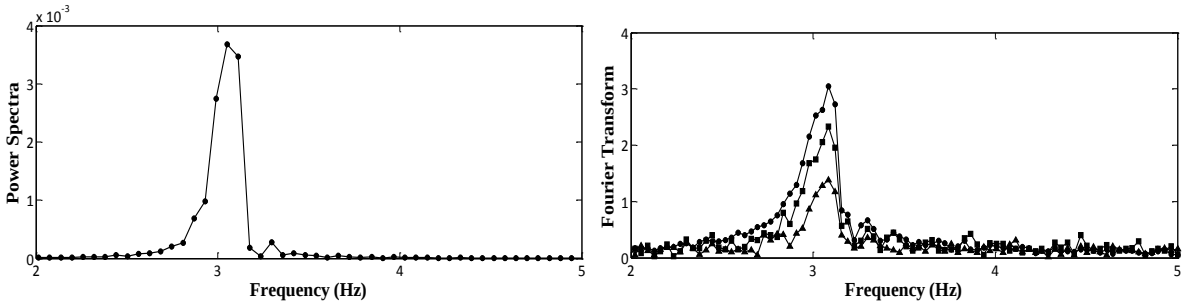

(a) Power spectra (b) Fast Fourier transform

Figure 5. Wall PTB-01 response

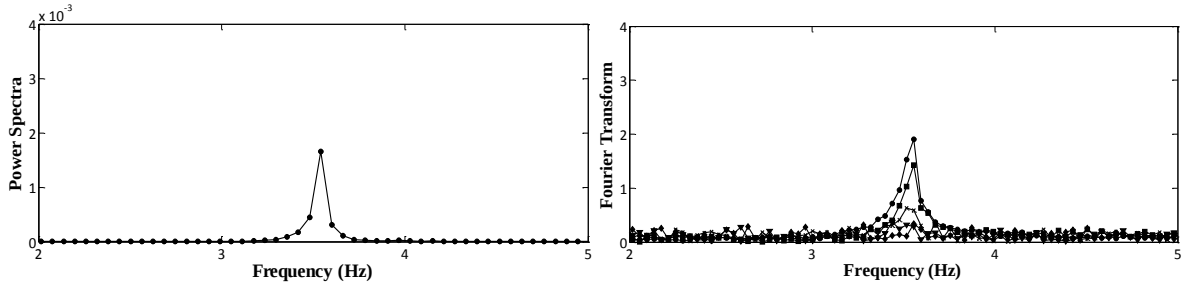

(a) Power spectra (b) Fast Fourier transform

Figure 6. Wall PTS-02 response

The fundamental modes of vibration of both walls were determined using stochastic subspace state space identification implemented in MATLAB and the results were compared with fast fourier transform and power spectra. The graphs for the fourier transform and the power spectra showed a peak in signal output which corresponded to the natural frequency of the walls. The natural frequency is represented by ω and the corresponding natural time period T of the walls was determined based on SDOF idealization. Table 4 shows the results of the tests.

Table 4. Dynamic test results

Wall designation	PTB-01	PTS-02
Natural Frequency-ω (Hz)	3.3	3.5
Natural Time Period-T (sec.)	0.30	0.28

3 NON-LINEAR STATIC ANALYSIS

3.1 Capacity Curve

Non-linear static analysis, also called pushover analysis, incorporates the non-linear force displacement characteristics of a building structure into an analytical model. A single degree of freedom (SDOF) idealization (see Figure 7) was used to formulate an idealized bi-linear pushover curve for URM walls retrofitted using posttensioning. For SDOF idealization the damping ratio is not directly considered, but is taken into account by using a damped response spectrum. Equation 1 represents a multi degree of freedom (MDOF) three dimensional model representing a building structure and when reduced to an equivalent undamped SDOF system the relation was reduced to Equation 3.

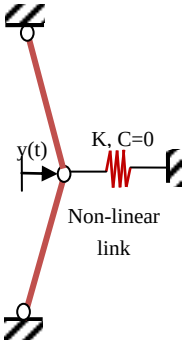

Figure 7. SDOF model

$$M\ddot{y}(t) + Ky(t) = F(t) \quad (3)$$

where, $y(t)=\frac{D_t}{\tau}, F(t)=\frac{F}{\tau}$ and τ is the modal participation factor that controls the transformation of a MDOF system to a SDOF system, D_t is the displacement and F is the applied external force. A bilinear response was presumed for the wall to define the non-linear behaviour, predicted by using strength based bilinear approximation that was previously advocated by Popehn et al. (2008). Equations 4 and 5 calculate the out-of-plane flexural capacity of posttensioned masonry walls where M_c and M_n represents the moments developed corresponding to crack penetration and yielding respectively.

$$M_c=\frac{I_n}{c}\left[f_r+\left(\frac{P_v+P_{sw}+A_{ps}f_{se}}{A_n}\right)\right] \tag{4}$$

$$M_n=\left(P_v+P_{sw}+A_{ps}f_{se}\right)\left[d_{eff}-\frac{\left(P_v+P_{sw}+A_{ps}f_{ps}\right)}{2\left(\lambda_n f_{bc} b\right)}\right] \tag{5}$$

Additional symbols used in Equations 4 and 5 are: I_n = net moment of inertia of masonry; c = distance of extreme compression fibre to neutral axis; f_r = modulus of rupture; P_v = overburden vertical load producing axial compression on masonry; P_{sw} = axial load due to self weight; A_{ps} = area of pre-stressing steel; f_{ps} = tensile stress in pre-stressing tendons at nominal strength; f_{se} = effective stress in pre-stressing tendons after all losses; A_n = net cross-sectional area of the masonry; d_{eff} = distance of extreme compression fibre to the centroid of tension reinforcement; b = width of cross section; λ_n = parameter representing the fraction of maximum compressive stress at nominal strength. Equation 6 was used to determine the corresponding displacement at crack penetration and was determined for a SDOF system with K_i being the initial stiffness of the wall in elastic range. A SDOF frame element, with fixed bottom and partial rotational restraint (see Figure 7), was analysed for incremental loading to produce the pushover capacity curve with Figure 8 showing the bilinear curve for test wall PTS-02 drawn using the SDOF model.

$$y(t)=\frac{F}{K_i} \tag{6}$$

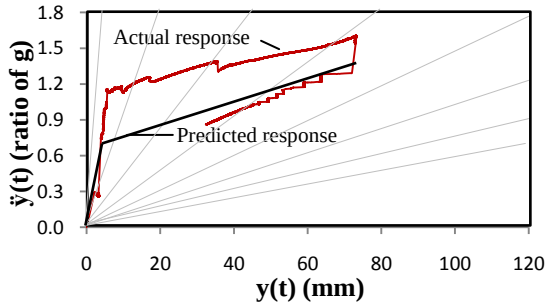

Figure 8. Bilinear wall response for PTS-02

As a single horizontal crack formed at wall mid-height when physically tested, it was presumed that a hinge was developed at mid-height. Therefore, the mid-height displacement (Δ) was considered critical and the analogous base shear (V) was plotted against the displacement at hinge location, referred to as a pushover curve in V-Δ format. An ultimate displacement capacity of 4% was adopted given that the tendon stress did not reach its yield strength. The V-Δ format push over curve was then transformed into spectral response acceleration and response displacement (ADRS) format using Equation 7, where W_{eff} is the effective weight of the wall.

$$C_s=\frac{V}{W_{eff}} \tag{7}$$

3.2 Demand Curve

It was assumed that a building was situated in Wellington and the earthquake parameters for the development of the elastic response spectrum were selected accordingly. The NZS 1170.5:2004 Loadings Standard was used to construct the elastic response spectrum in spectral acceleration period

format and the elastic response spectrum is shown in Figure 9. Equation 8 was used to transform the spectral acceleration *ÿ(t)* to spectral displacement *y(t)* and Figure 10 shows the spectral demand spectrum for the presumed site location.

$$y(t) = \frac{T^2}{4\pi^2}\ddot{y}(t) \qquad (8)$$

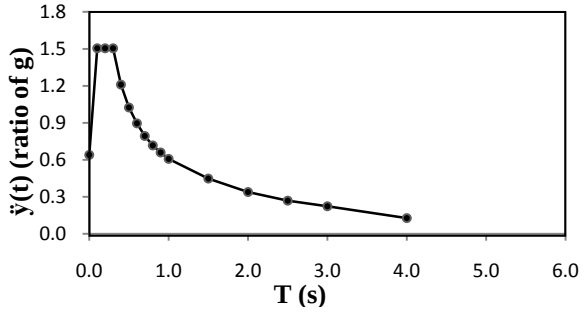

Figure 9. Elastic response spectrum

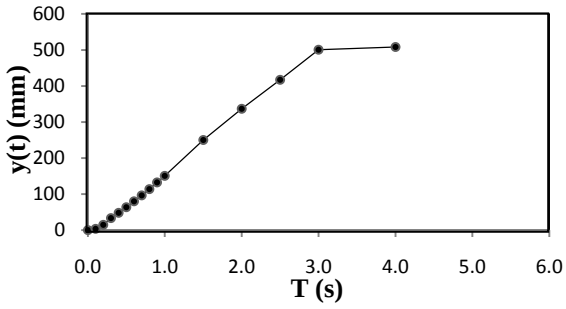

Figure 10. Displacement response spectrum

The values of spectral acceleration and spectral displacement against same period were used to construct demand spectra for different values of damping, with spectral acceleration on the Y-axis and spectral displacement on the X-axis, and the diagonal period lines radiating from the origin (ADRS format). Figure 11 shows the demand spectra for different damping values.

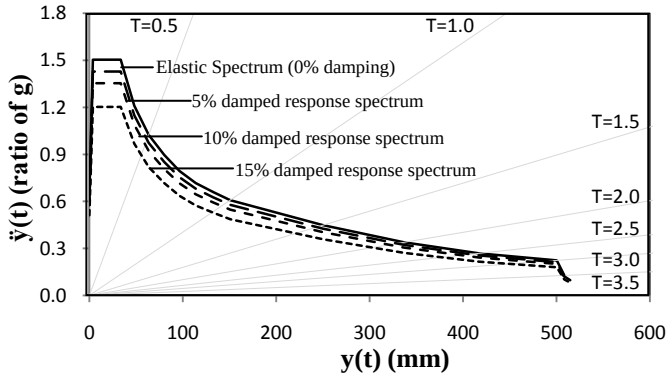

Figure 11. Demand spectra in ADRS format

3.3 Capacity Phase Diagram

A capacity phase diagram was drawn, plotting the 15% damped response spectrum (NZSEE 2006) and the pushover curve for the wall as detailed in section 3.2. The point where the capacity curve intercepts the demand curve was the expected maximum response of the wall. Figure 12 shows the capacity-demand curve for the wall and it was inferred from the diagram that the displacement of 49 mm and a base shear of 11.1 kN is the demand for the selected location.

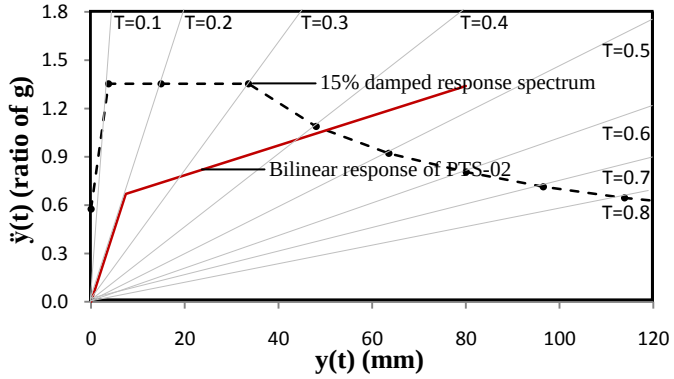

Figure 12. Capacity phase diagram

The proposed capacity phase diagrams can be used to design a posttensioning seismic retrofit solution

for URM walls by following the design steps:

1. Draw design demand spectra
2. Draw capacity curves for different levels of axial load
3. Select the optimum value of axial load
4. Calculate initial posttensioning force and centre to centre spacing of tendons, based on the tensile strength of tendons and the masonry compressive strength.

4 CONCLUSIONS

Existing equations to predict the out-of-plane (OOP) flexural capacity of posttensioned masonry walls were checked by comparing the predicted values to those obtained from OOP test results of two brick masonry walls seismically retrofitted using posttensioning. Also, the dynamic characteristics of natural frequency, mode shape and natural time period for the walls were determined by modal response tests. A single degree of freedom (SDOF) analytical model was developed using the pseudo-static and dynamic test results and was used to predict the capacity curve for the retrofitted walls. NZS 1170.5:2004 elastic response spectrum was used to generate the demand curve in spectral acceleration-spectral displacement (ADRS) format and a graphical method was used to predict the seismic behaviour of retrofitted walls. The method was found to predict anticipated quantitative damage in retrofitted URM walls for a design response spectrum. Test wall PTS-02 was analysed using the developed analysis procedure, with the initial prestress level as tested. It was inferred from the analysis results that the retrofitted URM wall would survive the design earthquake if the wall belongs to a URM building situated in Wellington.

5 ACKNOWLEDGMENTS

This research was conducted with financial support from Reid Construction Systems and the New Zealand Foundation for Research, Science and Technology. The Higher Education Commission of Pakistan provided funding for the doctoral studies of the first author. The authors are gratified to Faisal Shabbir, Hossein Derakhshan and Derek Lawley for help with the experimental setup.

REFERENCES

ATC. 1996. Seismic Evaluation and Retrofit of Concrete Buildings, Products 1.2 and 1.3 of the Proposition 122 Seismic Retrofit Practices Improvement Program (ATC-40). *SSC 96-01*, Applied Technology Council, California.

CEN. 1998. Eurocode 8 – Design provisions for earthquake resistance of structures. European Committee for Standardization, Brussels.

Chopra, A. K. and Goel, R. K. 1999. Capacity-demand-diagram methods based on inelastic design spectrum. *Earthquake Spectra*, 15(4), 637-656.

Derakhshan, H., Griffith, M.C., and Ingham, J.M. 2010. Airbag testing of unreinforced masonry walls subjected to one-way bending. *Journal of Structural Engineering*, in review.

Fajfar, P. 2000. A non linear analysis method for performance based seismic design. *Earthquake Spectra*, 16(3), 573-592.

Freeman, S. A. 1998. The capacity spectrum method as a tool for seismic design. In Proc. of *11th European Conference on Earthquake Engineering*, Paris, France, 6-11 September 1998.

Freeman, S. A., Nicoletti, J. P., and Tyrell, J. V. 1975. Evaluations of existing buildings for seismic risk– A case study of Puget Sound Naval Shipyard. In Proc. Of *1st U.S. National Conference on Earthquake Engineering*, Berkeley, 113-122.

Ismail, N., Laursen, P., and Ingham, J. M. 2009a. Out-of-plane testing of seismically retrofitted URM walls using posttensioning. In Proc. of *AEES 2009 Conference*, Newcastle, Australia, 11-13

December, 2009.

Ismail, N., Mahmood, H., Derakhashan, H., Clark, W., and Ingham, J. M. 2009b. Case study and development of retrofit application strategy for a heritage building. In Proc. Of *11th Canadian Masonry Symposium*, Toronto, Ontario, Canada, May 31-June 3, 2009.

Mogadam, A. S., and Tso, W. K. 2000. 3-D pushover analysis for damage assessment of buildings. *Journal of Seismology and Earthquake Engineering*, 2(3), 23-31.

NZSEE. 2006. Assessment and improvement of the structural performance of buildings in earthquakes : prioritisation, initial evaluation, detailed assessment, improvement measures : recommendations of a NZSEE study group on earthquake risk buildings, *New Zealand Society for Earthquake Engineering*, Wellington, N.Z.

Popehn, J. R. B., Schultz, A. E., Lu, M., Stolarski, H. K. and Ojard N. J. 2008. Influence of transverse loading on the stability of slender unreinforced masonry walls. *Engineering Structures*, 30(10), 2830-2839.

SANZ, 2004. NZS 1170; Structural Design Actions, Standards New Zealand, Wellington, New Zealand.